

PAPER • OPEN ACCESS

A Ship Radar Matching Method Based on Target Attributes and Point Pair Topological Characteristic

To cite this article: Jianan Wang *et al* 2021 *J. Phys.: Conf. Ser.* **2006** 012032

View the [article online](#) for updates and enhancements.

You may also like

- [A circular zone counting method of identifying a Duffing oscillator state transition and determining the critical value in weak signal detection](#)
Meng-Ping Li, , Xue-Mei Xu et al.
- [Robot motion visual measurement based on RANSAC and weighted constraints method](#)
Lulu Wu, Xianglin Deng, Yuan Wang et al.
- [Speeded-Up Robust Features-based image mosaic method for large-scale microscopic hyperspectral pathological imaging](#)
Qing Zhang, Li Sun, Jiangang Chen et al.



ECS
The
Electrochemical
Society
Advancing solid state &
electrochemical science & technology

DISCOVER
how sustainability
intersects with
electrochemistry & solid
state science research

A Ship Radar Matching Method Based on Target Attributes and Point Pair Topological Characteristic

Jianan Wang, Bo Wu*, Zhaojun Wang, Nana Yao, Jiajun Wu, Yue Gao

Space Star Technology CO.,LTD, Beijing, China

*Corresponding author's e-mail: wub@spacestar.com.cn

Abstract. We introduce a new ship target association method called SRM-AT, which stands for a Ship Radar Matching Method Based on Target Attributes and Point Pair Topological Characteristics. Using the radar properties of electromagnetic signals, as well as the longitude and latitude coordinates of electromagnetic signals and remote sensing images, this method calculates the point pair properties probability and PPTC (Point Pair Topological Characteristic) probability of electromagnetic signals and remote sensing images, as well as the syntheses of BPAF (Basic Probability Assignment Function) of the two through D-S evidence theory, to update the probability matrix of target association between electromagnetic signals and remote sensing images by using probability relaxation labelling method iteratively. The main contributions of this paper are: firstly, using decision trees to classify electromagnetic signals; finally, at the same time applicable to electromagnetic signals and remote sensing image ship formation and non-ship formation form. Through comparative experiments, this paper verifies that the method in this paper is superior to the comparative method in terms of association accuracy.

1. Introduction

Ocean target monitoring currently uses satellite collection of electromagnetic signal and remote sensing image as the main means. The collected electromagnetic signal covers a wide sea area and has high collection frequency, but its positioning accuracy is low. Therefore, the monitoring effect and even the decision-making will be seriously affected when the monitoring of ocean targets only relying on the electromagnetic signal. The collected remote sensing image has high positioning accuracy, less noise and small error, but it has high collection cost. Thence, only relying on remote sensing image for ocean target monitoring costs money and effort.

How to effectively improve the effect of ocean target monitoring is the ultimate goal of this paper. The ancients said: "listen to both sides, then dark." Only when the electromagnetic signal and the remote sensing image are organically combined, can better effects be achieved. Therefore, the integrated use of electromagnetic signal and remote sensing image can effectively solve this problem.

However, the above method faces many problems. For example, the collected electromagnetic signal is messy, and the remote sensing image has long time span, etc. Based on above, this paper proposes SRM-AT: a Ship Radar Matching Method Based on Target Attributes and Point Pair Topological Characteristic. The contributions of our paper are as follows:

- 1) The decision tree is used to classify electromagnetic signals.
- 2) At the same time, the ship formation and the non-ship formation of electromagnetic signal and remote sensing image data set are applicable.



2. Background Knowledge

2.1. Overview of the point pair topology characteristic

The ship target position of electromagnetic signal and remote sensing image can be regarded as two point modes on the plane, that is, each ship target position is regarded as a point in the point mode. Therefore, the ship target association between electromagnetic signal and remote sensing image can be transformed into the point matching problem which between two point modes. In this paper, the point pair topology based on the invariant characteristic of point set is used to describe the topological structure between ship targets, and the point matching is carried out by using the topological structure. The PPTC: Point Pair Topology Characteristic is defined as [1]:

As shown in Figure 1, point set $S (s_i, s_j \in S)$ has N points, and m_s is the centre of it. The PPTC $Pt_{ij}(s_i)$ of any s_j relative to another s_i is the spatial position: s_j relative to s_i in the polar coordinate system with s_i as the origin and $\overline{s_i m_s}$ as the positive axis, namely:

$$\left\{ \begin{array}{l} Pt_{ij}(s_i) = \{d(s_i, s_j), l(s_i, s_j) \mid s_i, s_j \in S; d(s_i, s_j) \in [1, p]; l(s_i, s_j) \in [1, q]\} \\ d(s_i, s_j) = k, (k-1)\Delta\rho < \log\rho - \log\min \leq k\Delta\rho \\ l(s_i, s_j) = k, (k-1)\Delta\theta_s < \angle s_j s_i m_s < k\Delta\theta_s \end{array} \right. \quad (1)$$

For two points $s_i=(x_i, y_i), s_j=(x_j, y_j)$ in the S , the PPTC $Pt_{ij}(s_i)$ of s_j relative to s_i can be calculated by the following formula:

$$\left\{ \begin{array}{l} Pt_{ij}(s_i) = \{d(s_i, s_j), l(s_i, s_j)\} \\ d(s_i, s_j) = \frac{\log\rho - \log\min}{(\log\max - \log\min)} \times p \\ l(s_i, s_j) = \frac{\angle s_j s_i m_s}{360^\circ} \times q \end{array} \right. \quad (2)$$

In formula (1) and (2), $d(s_i, s_j)$ represents the quantized distance of s_j and s_i ; $l(s_i, s_j)$ denotes the quantized angle of counterclockwise rotation with $\overline{s_i s_j}$ respect to $\overline{s_i m_s}$, p and q mean the point set space of s_i divided into p intervals by logarithmic distance $\log\rho$ and q intervals by angle θ , $\Delta\rho = \lfloor (\log\max - \log\min) / p \rfloor$, $\Delta\theta_s = \lfloor 360^\circ / q \rfloor$, $\angle s_j s_i m_s$ represents the counterclockwise rotation angle of $\overline{s_i s_j}$ relative to $\overline{s_i m_s}$. ρ is the spherical distance between s_i and s_j . Max and min respectively represent the spherical distance between s_i and another point with the longest and the nearest distance.

It can be proved that: given a fixed point set S , the point set $T(t_i, t_j \in T)$ is obtained through the similarity transformation of S , then the PPTC of $S(s_j$ relative to $s_i)$ and $T(t_j$ relative to $t_i)$ are the same, that is, the PPTC has the similarity transformation invariance.

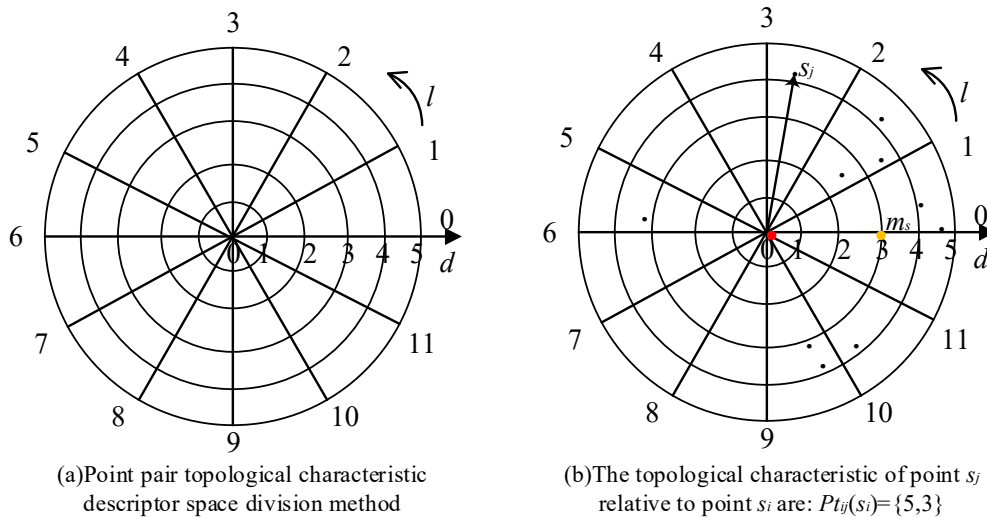


Figure 1. Description of topological characteristic on point pairs

2.2. D-S evidence theory

D-S evidence (Dempster-Shafer) theory is a set of mathematical methods based on "evidence" and "combination" to deal with uncertain reasoning problems, which is widely used in information fusion, multi-attribute decision analysis and other fields. The core of D-S evidence theory is evidence synthesis formula, whose definition is shown in formula (3)[2]:

$$m(X) = \frac{\sum_{X_{1i_1} \cap X_{2i_2} = X} m_1(X_{1i_1}) m_2(X_{2i_2})}{1 - \sum_{X_{1i_1} \cap X_{2i_2} = \Phi} m_1(X_{1i_1}) m_2(X_{2i_2})}, \forall X \in \Theta, X \neq \Phi \tag{3}$$

Among them, Θ is the recognition framework, $X_{11}, X_{12}, \dots, X_{1K}$ and $X_{21}, X_{22}, \dots, X_{2L}$ mean the focal element, m_1 and m_2 are the trust function, m represents the S-BPAF, which stands for the Syntheses of Basic Probability Assignment Function (m satisfies formula (4)).

$$\sum_{A \subseteq \Theta} m(A) = 1, \quad m(\Phi) = 0 \tag{4}$$

In formula (3), if $\sum_{X_{1i_1} \cap X_{2i_2} = X} m_1(X_{1i_1}) m_2(X_{2i_2}) \neq 1$, then we can say that m can determine a S-BPAF; if $\sum_{X_{1i_1} \cap X_{2i_2} = X} m_1(X_{1i_1}) m_2(X_{2i_2}) = 1$, it is considered that m_1 and m_2 completely conflict, and the S-BPAF cannot be obtained.

3. Algorithm of SRM-AT

3.1. Similarity matching metric of point pair topological characteristic

The PPTC is invariant feature under similarity transformation, it has strong robustness to noise and outliers. In this paper, PPTC is used to calculate the similarity matching metric of point set. The specific method is as follows:

In point set S , the PPTC of s_i relative to s_j is as follows:

$$Pt_{ij}(s_i) = \{d(s_i, s_j), l(s_i, s_j) | s_i, s_j \in S; d(s_i, s_j) \in [1, p]; l(s_i, s_j) \in [1, q]\} \tag{5}$$

In point set T, the PPTC of t_i relative to t_j is as follows:

$$Pt_{ij'}(t_i) = \{d(t_i, t_j), l(t_i, t_j) \mid t_i, t_j \in T; d(t_i, t_j) \in [1, p]; l(t_i, t_j) \in [1, q]\} \quad (6)$$

According to formula (5) and formula (6), the similarity matching metric between PPTC of (s_i, s_j) in S and (t_i, t_j) in T can be defined as follows:

$$\begin{cases} \alpha = \exp\left(-\frac{|d(t_i, t_j) - d(s_i, s_j)|}{\max_{i, j \in [1, m]} \{d(s_i, s_j), d(t_i, t_j)\}} / \sigma_\alpha^2\right) \\ \beta = \exp\left(-\frac{|l(t_i, t_j) - l(s_i, s_j)|}{\max_{i, j \in [1, m]} \{l(s_i, s_j), l(t_i, t_j)\}} / \sigma_\beta^2\right) \\ C_{ij, i'j'} = (1 - \alpha) \cdot (1 - \beta) \end{cases} \quad (7)$$

In formula (7), α and β respectively indicate the similarity of the distance and the angle. σ_α and σ_β represent the distance and the angle limiting coefficient, respectively. $C_{ij, i'j'}$ denotes the degree of similarity between the topological characteristic of s_i relative to s_j and that of t_i relative to t_j . The smaller $C_{ij, i'j'}$ is, the more similar the PPTC of s_i relative to s_j and the PPTC of t_i relative to t_j .

3.2. Basic probability assignment function based on point pair topology characteristic

The ship set composed of N ship targets can be equivalent to the point mode with size N. Any point (any ship target) in the point mode can obtain N-1 point pair topological characteristics, so the whole point mode (ship set) can obtain $N \times (N-1)$ point pair topological characteristics. In this paper, the BPAF, which stands for Basic Probability Assignment Function is constructed by the similarity matching metric which based on the topological characteristics of two point sets, so that the matching problem of electromagnetic signal and remote sensing image can be realized by using the PPTC.

To sum up, the BPAF based on PPTC can be expressed by formula (8):

$$Op(s_i, s_j, t_i, t_j) = \frac{1}{1 + (C_{ij, i'j'} + C_{ji, j'i'})^2} \quad (8)$$

$Op(s_i, s_j, t_i, t_j)$ is the compatibility of point pair (s_i, t_i) and point pair (s_j, t_j) , a value of 1 represents the maximum compatibility between the two point pairs, and 0 means the two point pairs are incompatible. The BPAF satisfies the requirement of compatibility coefficient, and can enhance the robustness to positioning error and false alarm.

3.3. Calculate the matching probability function of unknown radar

Suppose the electromagnetic signal set is $S = \{s_1, s_2, \dots, s_n\}$; the feature vector E is constructed by the carrier frequency, pulse repetition frequency and pulse width attributes of the detected N radiation sources; suppose the set of ship remote sensing image is $T = \{t_1, t_2, \dots, t_n\}$. M radar categories can be obtained by inputting E into the decision tree classifier, and then the ship type of the M radars can be determined through the "ship-radar" classification information database.

The reasoning judgment from electromagnetic signal to remote sensing image can be determined according to the ship remote sensing image and the ship-radar allocation library. Set the identification results of the electromagnetic signal $S_i (i = 1, 2, \dots, i, \dots, n)$ are:

$$P^{S_i} = \{P_{W_1}^{S_i}, P_{W_2}^{S_i}, \dots, P_{W_M}^{S_i}\} \tag{9}$$

In formula (9), if the electromagnetic signal S_i is identified as the radar W_j , then $P_{W_j}^{S_i} = 1$, otherwise $P_{W_j}^{S_i} = 0$.

Suppose the probability that the $W_j (j=1,2,\dots,M)$ radar carried on the k -th($k=1,2,\dots,M$) ship remote sensing image is expressed as $P_{t_k}^{W_j}$. In the ship-radar allocation library, M -type ships carrying W_j appeared in the set of ship remote sensing image can be expressed as $\{h_1^{W_j}, h_2^{W_j}, \dots, h_M^{W_j}\}$. This paper uses $\{h_1^{W_j}, h_2^{W_j}, \dots, h_M^{W_j}\}$ to determine $P_{t_k}^{W_j}$, that is, if $h_k^{W_j}$ is true, then $P_{t_k}^{W_j}$ is 1, otherwise it is 0. The probability $P_{h_k}^{W_j}$ of the ship h_k carrying W_j satisfies the following formula:

$$P_{h_k}^{W_j} = \frac{h_k^{W_j}}{\sum_{k=1}^M h_k^{W_j}} \tag{10}$$

The probability that the target S_i belongs to the k -th ($k=1, 2, \dots, M$) ship remote sensing image t_k is:

$$P_{t_k}^{S_i} = P_{W_j}^{S_i} \cdot P_{h_k}^{W_j} \tag{11}$$

After the target S_i is classified and identified by the radar radiation source, this paper calculates the recognition result according to the ship-radar allocation library, and the recognition result can be expressed as:

$$P^{S_i} = \{P_{t_1}^{S_i}, P_{t_2}^{S_i}, \dots, P_{t_m}^{S_i}\} \tag{12}$$

3.4. Initialize the association probability matrix

Since the PPTC and the attribute feature are independent of each other, they can be used as two evidences to judge whether electromagnetic signal and remote sensing image are associated. According to formula (3), the BPAF corresponding to the PPTC and point pair attribute feature can be combined to obtain the S-BPAF. The S-BPAF can be used to initialize the association probability matrix.

The BPAF $Op(s_i, s_j, t_{i'}, t_{j'})$ based on PPTC is shown in formula (8). Let the BPAF based on attribute feature be $Ep(s_i, s_j, t_{i'}, t_{j'})$, and the calculation method is as follows:

$$Ep(s_i, s_j, t_{i'}, t_{j'}) = r_{i'j'} \cdot r_{jj'} \tag{13}$$

$$r_{i'j'} = P_i^{Et_{i'}} \tag{14}$$

Based on the above conditions, evidence synthesis can be carried out to obtain the S-BPAF $C(s_i \leftrightarrow t_{i'}, s_j \leftrightarrow t_{j'})$:

$$C(s_i \leftrightarrow t_{i'}, s_j \leftrightarrow t_{j'}) = \frac{\sum_{\alpha=(s_{i1} \leftrightarrow t_{i'1}, s_{j1} \leftrightarrow t_{j'1})} Op(s_{i1}, s_{j1}, t_{i'1}, t_{j'1}) * Ep(s_{i2}, s_{j2}, t_{i'2}, t_{j'2})}{1 - \sum_{\alpha=\emptyset} Op(s_{i1}, s_{j1}, t_{i'1}, t_{j'1}) * Ep(s_{i2}, s_{j2}, t_{i'2}, t_{j'2})} \tag{15}$$

Among them:

$$\alpha = (s_{i1} \leftrightarrow t_{i'1}, s_{j1} \leftrightarrow t_{j'1}) \cap (s_{i2} \leftrightarrow t_{i'2}, s_{j2} \leftrightarrow t_{j'2}) \tag{16}$$

The ship target positions of remote sensing image and electromagnetic signal are used as target set and template set respectively. Set the target set $T = \{t_{i'} | i' = 1, 2, \dots, n_i\}$, where $t_{i'} = (x_{i'}, y_{i'})$; template set $S = \{s_i | i = 1, 2, \dots, n_s\}$, where $s_i = (x_i, y_i)$. Target association aims to find the best association result from the target set and the template set, that is, $r: s_i \rightarrow t_{r(i)}$, where $r(i) = i'$. In the mathematical model, the

association probability matrix $A=[A_{ii'}]_{n_s \times n_t}$ is used to describe the point pair association degree between the target set and the template set, where $A_{ii'} (i \in [1, 2, \dots, n_s]; i' \in [1, 2, \dots, n_t])$ is the association probability between s_i and $t_{i'}$.

Let the initial association probability matrix be $A^{(0)}=[A_{ii'}^{(0)}]_{n_s \times n_t}$, where $A_{ii'}^{(0)}$ is the initial probability of $s_i \leftrightarrow t_{i'}$ (s_i and $t_{i'}$ associated). When $s_i \leftrightarrow t_{i'}$, for any $s_j (j \neq i)$, it is hoped that there is and only a unique $t_{j'} (j' \neq i')$ associated with it, so $\max_{j' \neq i'} [C(s_i \leftrightarrow t_{i'}, s_j \leftrightarrow t_{j'})]$ can be used to represent the support of $s_j \leftrightarrow t_{j'}$ to $s_i \leftrightarrow t_{i'}$.

To sum up, the initial association probability $A_{ii'}^{(0)}$ of $s_i \leftrightarrow t_{i'}$ is the mean value of all possible $s_j \leftrightarrow t_{j'}$ support to $s_i \leftrightarrow t_{i'}$ ($j \neq i, j' \neq i'$), namely:

$$A_{ii'}^{(0)} = \frac{1}{n-1} \sum_{j \neq i} \{ \max_{j' \neq i'} [C(s_i \leftrightarrow t_{i'}, s_j \leftrightarrow t_{j'})] \} \quad (17)$$

Where $1 \leq i \leq n_s, 1 \leq i' \leq n_t$.

3.5. Relaxation labeling optimization

Relaxation labeling method describes targets by using markers. This method first gives a set of initial markers for the targets, then updates the markers successively through iterative operation, and finally obtains the exact set of markers for the corresponding targets. This paper uses relaxation labeling method to find the optimal target association probability matrix [3].

In the optimization process of relaxation labeling method, for the r-th iteration, the support of $s_j \leftrightarrow t_{j'}$ to $s_i \leftrightarrow t_{i'}$ is not only related to the compatibility metric of $s_i \leftrightarrow t_{i'}$ and $s_j \leftrightarrow t_{j'}$ (syntheses of basic probability assignment function $C(s_i \leftrightarrow t_{i'}, s_j \leftrightarrow t_{j'})$), but also need to consider the $A_{jj'}^{(r-1)}$. Therefore, taking the maximum value of the above two minimums indicates the support of $s_j \leftrightarrow t_{j'}$ to the $s_i \leftrightarrow t_{i'}$. Thus, the iterative updating formula of the association probability matrix is:

$$A_{ii'}^{(r)} = \frac{1}{n-1} \sum_{j \neq i} [\max_{j' \neq i'} \{ \min [C(s_i \leftrightarrow t_{i'}, s_j \leftrightarrow t_{j'}), A_{jj'}^{(r-1)}] \}] \quad (18)$$

In order to meet the one-to-one matching constraint, the association probability matrix must be regularized in columns and rows after each iteration, so that $\forall i \in [1, 2, \dots, n_s]$, all have $\sum_{i'=1}^{n_t} A_{ii'}^{(r)} = 1$.

The iterative end condition of the relaxation labeling method is the association probability matrix A converges, that is, the difference between the k-th and the k-1th iteration results is less than the given threshold ε :

$$\delta(k) = \|A^{(k)} - A^{(k-1)}\| < \varepsilon \quad (19)$$

At this point, the optimal association matrix A satisfying the one-to-one matching constraint can be obtained.

4. Experiment and analysis

4.1. Experimental setup

In order to verify the effectiveness of the SRM-AT, two sets of comparative experiments are set up in this section. The first set of experiments compares ICP[4], PPLT-PRL[5], SM[6], SVD[7], PPTC-SM[1], PPTC-PRL[1] and the SRM-AT algorithms. The performances of these algorithms are compared on the ship formation set data of random affine transformation. The second set of experiments uses real non-ship formation (inter-ships independent of each other) data set provided by Party X to verify the practical effectiveness of the SRM-AT. In the two sets of experiments, the parameters of SRM-AT are set as: distance interval P =5, angle interval Q =12; distance limiting coefficient and angle limiting coefficient are both 1.1.

Experiment (I): The related algorithms are compared with the performance of anti-rotation, positioning error adaptability and anti-false alarm on the random affine transformed ship formation set data. The PPTC calculation stage uses remote sensing image latitude and longitude coordinate data to generate a target set, and the template set is generated through random affine transformation. The target set is composed of: $\{(25,15); (12,30); (15,47); (40,15); (40,25); (40,40); (40,75); (70,30); (70,65)\}$. The random affine transformation matrix \mathbf{H} can be expressed by formula (20).

$$\mathbf{H} = \alpha \begin{bmatrix} \cos \theta & \sin \theta & t_x \\ -\sin \theta & \cos \theta & t_y \\ 0 & 0 & 1 \end{bmatrix} \quad (20)$$

The meaning and the value of each parameter in formula (20) are as follows:

Scale factor $\alpha: 0.1 \leq \alpha \leq 5.0$, which is fixed as 1 in this paper; rotation angle $\theta: -180^\circ \leq \theta \leq 180^\circ$ (in the anti-rotation comparison experiment, rotation angle is taken at intervals of 60 angle); displacement parameter t_x, t_y are both 0.3, $-0.5 \leq t_x, t_y \leq 0.5$. For the positioning error adaptability comparison experiment, this paper adds the mean value of 0 to the longitude and latitude coordinate of each point in the template set, and the variance is the Gaussian noise of f times the minimum Euclidean distance between two points in the template set, where f is the positioning error level factor. In the anti-false alarm comparison experiment, this paper randomly adds $r \times N_s$ false points to the template set, where r is the out-of-grid point rate and N_s is the number of template set point.

In experiment (II), the longitude and the latitude coordinates of real remote sensing image and electromagnetic signal provided by the X party constitutes the target set and the template set required by the PPTC stage. We randomly selects 5, 8 and 11 data points for analysis experiment. In experiment (II), the algorithms involved in comparison include ICP, PPLT-PRL, SM and SVD.

4.2. Experimental results

4.2.1. Experiment I: The experimental results are shown in Figure 2, 3, and 4.

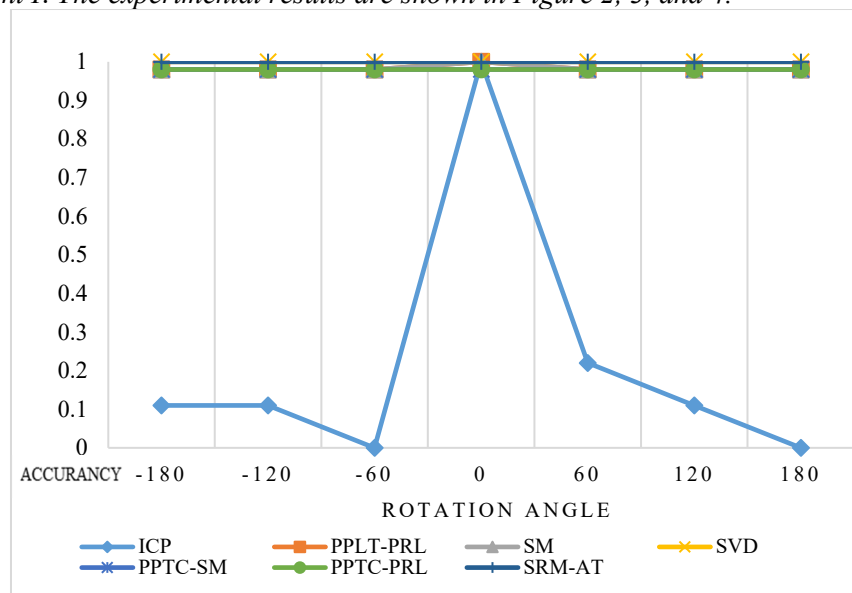


Figure 2. experimental results

Figure 2 shows the anti-rotation performance of SRM-AT and other six algorithms. The ordinate is the matching accuracy of these algorithms, and the abscissa is the rotation angle. When the rotation angle is 0, the accuracy of various algorithms is 100%. As the rotation angle decreases or increases, except for SM, PPTC-SM, PPTC-PRL and SRM-AT, the accuracy of other algorithms fluctuates greatly. Among

them, the accuracy of ICP fluctuates the most, indicating that the algorithm presented in this paper has rotation invariance, and the anti-rotation performance of ICP is poor.

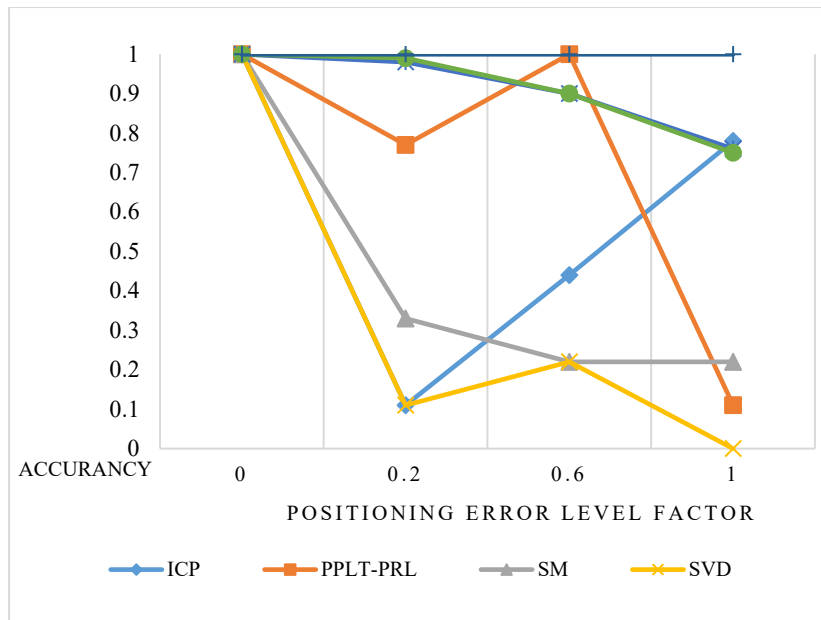


Figure 3. experimental results

Figure 3 shows a line chart of matching accuracy of the seven algorithms. The ordinate is the algorithm matching accuracy and the abscissa is the positioning error level factor. Observing Figure 3, we can get: the SRM-AT is most adaptable to positioning error, and its accuracy rate is 100%. The matching accuracy of PPTC-SM and PPTC-PRL is always higher than 75%, showing that they have strong adaptability to positioning error. The accuracy of SM and SVD decreases with the increasing of positioning error factor, so their adaptability to positioning error is poor, while ICP and PPLT-PRL are not suitable for the setting with large positioning error factor.

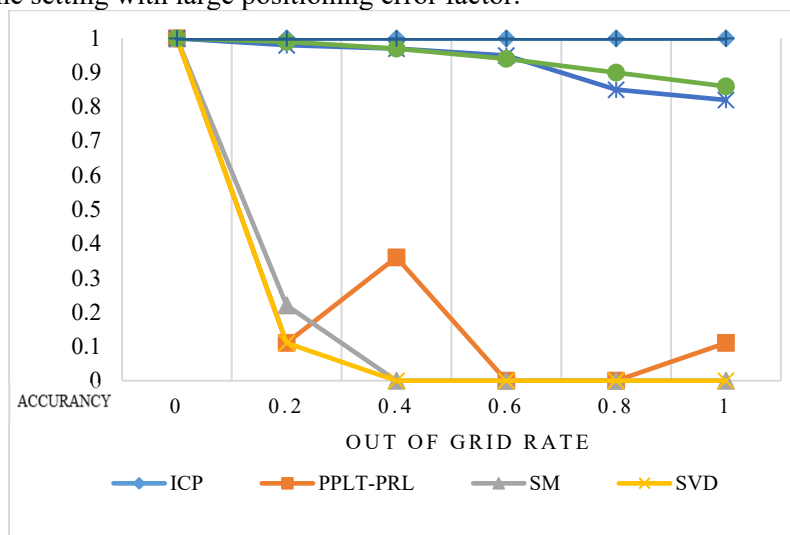


Figure 4. experimental results

Figure 4 shows a line chart of matching accuracy and out-of-grid rate, the algorithms involved in the experiment are ICP, PPLT-PRL, SM, SVD, PPTC-SM, PPTC-PRL and the SRM-AT. The vertical axis is matching accuracy and the abscissa is out-of-grid rate. In Figure 4, the accuracy of SVD and SM decreases as the out-of-grid rate increasing. When the out-of-grid rate is 0.4, the accuracy of SVD and

SM is reduced to 0. The anti-false alarm performance of ICP and PPLT-PRL is unstable, and their accuracy fluctuates greatly due to the influence of out-of-grid rate. PPTC-SM and PPTC-PRL are both more accurate than 80%, and their anti-false alarm performance is strong, but still weaker than the algorithm in this paper: SRM-AT is not affected by out-of-grid rate and has an accuracy of 100%.

4.2.2. *Experiment II.* Figure 5 shows the comparison results of ICP, PPLT-PRL, SM, SVD, and SRM-AT on the data of real non-ship formation (ships are independent of each other).

The ordinate is matching accuracy, and the absciss represents the number of target and template adopted in the experiment. It can be concluded that SRM-AT has the highest matching accuracy in the real data. In experiments with target and template set of 5×5 , 8×8 , and 11×11 , the matching accuracy of SRM-AT is 80%, 50%, and 73%, far higher than that of PPLT-PRL and ICP (23% and 12%, respectively). The experimental results show that SRM-AT has strong practical feasibility, while SM and SVD are less feasible, and are not suitable for non-ship formation data.

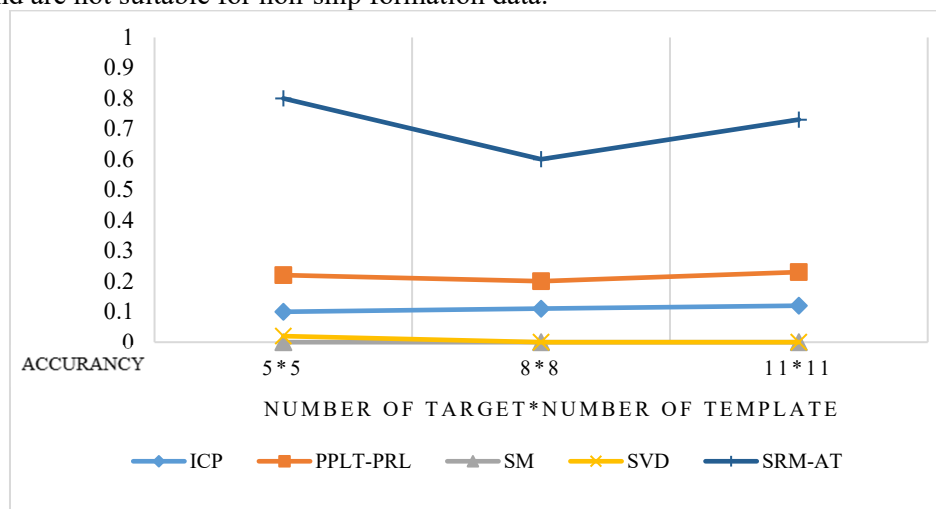


Figure 5. experimental results

4.3. Experimental analysis

Analysis of the experimental results of Section 4.2 shows that the anti-rotation performance, adaptability to positioning error and anti-false alarm performance of SRM-AT are superior to other algorithms. The reasons are as follows:

ICP realizes target association by iteratively searching for the nearest point, but it lacks adaptability to geometric deformation. Therefore, when the geometric deformation of the associated target is large, the target association performance of ICP will be weakened, as shown in the following: in experiments of anti-rotation and adaptability to positioning error, the matching accuracy of ICP is low and the fluctuation range is large. PPLT-PRL achieves target association based on point-to-local features, and has rich deformation description ability, but its local deformation invariance is sensitive to out-of-grid point and positioning error. Therefore, the PPLT-PRL has a low matching accuracy in the experiment of anti-false alarm and adaptability to positioning error. SM achieves point matching by calculating distance matrix and singular value decomposition, and is suitable for scenes with rotation, positioning error and out-of-grid point. However, SM is sensitive to scaling, so its performance is poor when setting scaling factor. SVD performs point matching based on measurement matrix, singular value decomposition and decision matrix, and is suitable for similar transformation scenarios. However, SVD is sensitive to positioning error and out-of-grid point, and therefore performs well only in anti-rotation experiment. PPTC-SM and PPTC-PRL are based on the above four algorithms, so they are superior to the other four algorithms in terms of anti-rotation, adaptability to positioning error and anti-false alarm. SRM-AT uses target radar attributes and location information to achieve target association, which fully

integrates the advantages of attribute characteristics and point-to-topological characteristics, so the performance is superior to other algorithms.

We can see that SRM-AT is highly adaptable to rotation, positioning error and false alarm. Therefore, under the real data of experiment (II), its performance is obviously better than that of other methods. ICP, PPLT-PRL, SM and SVD have their own shortcomings in geometric deformation, positioning error adaptability and anti-false alarm, so their performance under real data condition is low.

5. Related work

According to different correlation factors, target association can be realized based on[8]: (a)attribute information; (b)location information; (c)fusion of attribute and location information. Target association based on attribute information judges matching relationship between targets according to the degree of agreement between attributes [9-11], it has better performance in some specific problems, but the generalization performance is poor. Target association based on location information can be divided into methods based on motion state information and point pattern matching. Target association based on motion state information uses the periodic output of active observation periodic scanning to extract the target position information and estimate the motion state of the target, so as to achieve the purpose of target association [12, 13]; The method based on point pattern matching considers the target location information as a point pattern and uses the matching relationship between point patterns to achieve the target association. The typical methods include: Point Pair Topological Characteristics and Probability Relaxation Labeling(PPTC-PRL)[1], Point Pair Topological Characteristics and Spectral Matching(PPTC-SM)[1]. Both of them make use of the invariable features in the ship formation and match the target with the probability relaxation labelling method and spectral matching method respectively. Target association based on location information is mature, but it is not suitable for situations with low information revisit rate. Different from the above mentioned method, which uses a single feature, the target association method that combines location and attribute information uses the complementarity between target location information and attribute information to construct the comprehensive association discriminant function in order to achieve the goal of association. For example, the TBM global distance measure for the association of uncertain combat ID declarations[14], and the target association method based on topology and attribute feature[1], etc. The TBM global distance measure for the association of uncertain combat ID declarations is based on D-S evidence theory, proposed under the background of high information revisit rate, which is not applicable to the scenario with low information revisit rate. The target association method based on topology and attribute feature uses D-S evidence theory to combine the topological feature and attribute feature, which can correct the defects when using a single feature for target association, however, it is not applicable to the scenarios between non-ship formation.

6. Conclusion

In order to improve the accuracy of target association method, this paper proposes a Ship Radar Matching Method Based on Target Attributes and Point Pair Topological Characteristic, called SRM-AT. This method utilizes the advantages of attribute feature and PPTC, and after fusing the two through D-S evidence theory, the relaxation labeling method is used to obtain the optimal matching result of the target. Through comparative experiments, we see that when the data has rotation angle, positioning error or false alarm rate, the association effect of SRM-AT is far superior to the method that only uses topological or attribute characteristic, which verifies the effectiveness of the method in this paper.

Acknowledgement

This research was supported by the Space Star Technology CO., LTD.

References

- [1] L. Chunyan, (2012)Ship Targets Association Based on Satellite Electronic and Imaging

- Reconnaissance Information , master, National University of Defense Technology.
- [2] Dempster and P. A., (1967)Upper and Lower Probabilities Included by a Multivalued Mapping,Annals of Mathematical Stats, vol. 38, no. 2, pp. 325-339, 1967.
 - [3] Z. Jian, S. Jixiang, L. Zhiyong, and C. Mingsheng, (2011)Point pattern matching algorithm based on relative shape context and probabilistic relaxation labeling, Signal Processing, vol. 27, no. 5, pp. 664-671.
 - [4] P. J. Besl and O. Hasegawa, (1992)A method for registration 3-D shapes, IEEE Trans.pattern Anal.mach.intell, vol. 14, no. 2, pp. 193-200.
 - [5] D. Wanxia, (2016)Ship Target Correlation based on satellite image information and electronic information, National University of Defense Technology.
 - [6] M. Leordeanu and M. Hebert, (2005)A spectral technique for correspondence problems using pairwise constraints, in Tenth IEEE International Conference on Computer Vision.
 - [7] L. S. Shapiro and J. M. Brady, (1992)Feature-based correspondence: An eigenvector approach, Image and Vision Computing, vol. 10, no. 5, pp. 283-288,.
 - [8] Z. Hao, (2008)Data association research about targets among ship formation based on heterogeneous spaceborne reconnaissance sensors , National University of Defense Technology.
 - [9] Y. Bar-Shalom, T. Kirubarajan, and C. Gokberk, (2005)Tracking with classification-aided multiframe data association, IEEE Transactions on Aerospace & Electronic Systems, vol. 41, no. 3, pp. 868-878.
 - [10] Y. Hongwen, H. Weidong, and Y. Wenxian, (2008)Group target data association algorithm based on space distribution feature, Journal of System Simulation, no. 22, pp. 6074-6077.
 - [11] W. Jiyang, L. Jun, and S. Yi, (2006)A multi-target association algorithm based on analysis of terrain, Fire Control and Command Control, vol. 31, no. 10.
 - [12] A. M. Aziz, M. Tummala, and R. Cristi, (1999)Fuzzy logic data correlation approach in multisensor-multitarget tracking systems, Signal Processing .
 - [13] T. Denux, (1995)A k-nearest neighbor classification rule based on Dempster-Shafer theory, Systems Man & Cybernetics IEEE Transactions on, vol. 25, no. 5, pp. 804-813.
 - [14] B. Ristic and P. Smets, (2014)The TBM global distance measure for the association of uncertain combat ID declarations, Information Fusion, vol. 7, no. 3, pp. 276-284 .